THE USE OF STREAMWISE VORTICITY TO INCREASE MASS ENTRAINMENT IN A CYLINDRICAL EJECTOR

M.J. Carletti and C.B. Rogers*
Tufts University
Medford, Massachusetts

D.E. Parekh**
McDonnell Douglas Corporation
St. Louis, Missouri

Abstract

The following work documents the effect of streamwise vortices generated at the nozzle exit of an axisymmetric air jet on the amount of mass entrained into an ejector. In an experimental analysis of the mass entrainment of circular jet ejectors, we found that the introduction of half delta wing vortex generators in the exit of the jet nozzle (Reynolds number of 50,000) increased the amount of entrained mass by as much as 35% over the amount of increase provided by the ejector alone. The effectiveness of the generators was studied for several cases varying spacing, diameter, length, and Reynolds number. Although the performance of an ejector is a strong function of these parameters, the mass entrainment increased in all cases studied due to the presence of the vortex generators.

Nomenclature

Ae	- ejector area
Aj	- jet area
De	- ejector diameter
Dj	- jet diameter
Le	- ejector length
$\dot{m}$	- mass flow rate
$\dot{m}_{ejector}$	- mass exiting the ejector
$\dot{m}_{entrained}$	- mass entrained into the ejector
$\dot{m}_{nozzle}$	- mass exiting the jet nozzle
Re	- Reynolds number
ref	- reference case
S	- distance from jet to ejector
vor	- vortex case
$\overline{U}$	- time averaged velocity
$\overline{U}_{ejector}$	- average velocity exiting ejector
$\overline{U}_{nozzle}$	- average velocity exiting jet nozzle
$\overline{U}_{plenum}$	- average velocity based on jet plenum pressure
η	- increase in mass entrainment due to the generators
ρ	- fluid density

---

* Assistant Professor, Member AIAA
** Scientist, Member AIAA

General Introduction

Over the past forty years, several experimental and analytical studies have been conducted on the thrust augmentation characteristics of jet ejectors. An ejector is a relatively simple pumping device with no moving parts. Using the kinetic energy of the primary flow, an ejector causes a pressure drop which induces the flow of a low energy secondary stream into the ejector. The mixing of the two flows reduces the velocity of the jet within the ejector shroud, while increasing the exiting mass flux. By increasing the mass flow rate through the ejector, an increase in thrust can be attained. Since the overall velocity exiting the ejector is reduced, and jet noise is proportional to the exit velocity to the eighth power at subsonic and transonic Mach numbers, the noise generated can also be substantially decreased. Finally, the entrainment of ambient air reduces the overall temperature of the exhaust, thus reducing aircraft IR signatures.

Since the performance of an ejector is dependent on the efficient transfer of energy between the primary and secondary flows, current research has focused on the improvement of mixing within the ejector shroud. For most aeronautical applications, the mixing of the core flow must occur within a minimum distance so that unnecessary losses due to friction and weight can be avoided. Although the performance of a larger ejector may be superior, the increase in drag associated with this additional size must be taken into account in terms of practicality and design.

Recent studies have been very successful in enhancing the mixing characteristics of ejectors by introducing vorticity at the exit of the jet nozzle. Using a mixer ejector designed to introduce an array of large-scale, low-intensity streamwise vortices at the exit of a rectangular primary nozzle, Tillman et. al. have achieved well-mixed exit flows within two duct diameters [1] 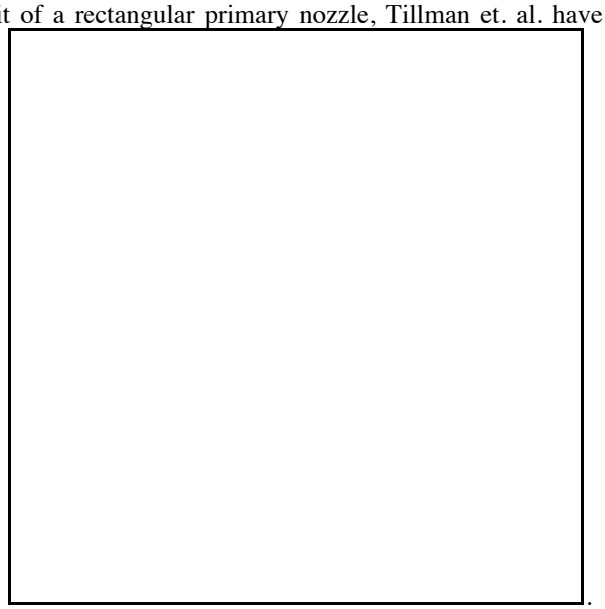 . The current design incorporates large scale streamwise vorticity, which stirs the flow rather than relying on the shear mixing 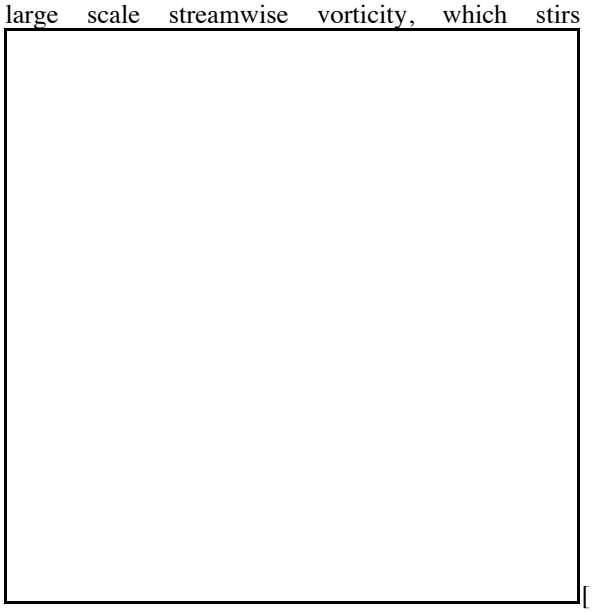 [1-5] 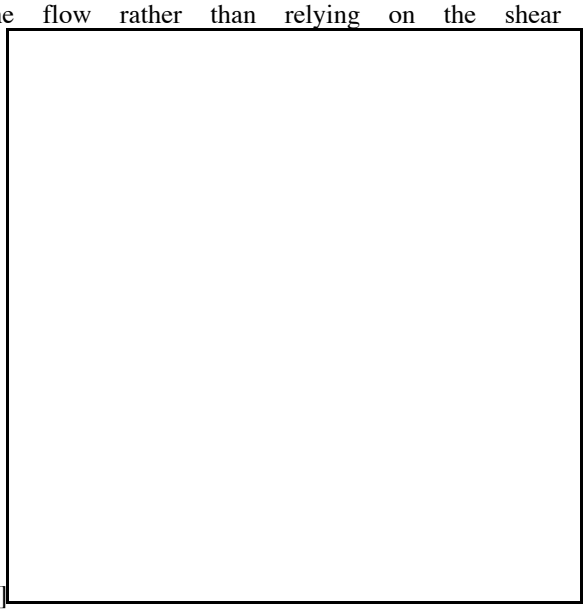 . It has been shown to be more effective than the previously studied small, intense streamwise vorticity used in hypermixing

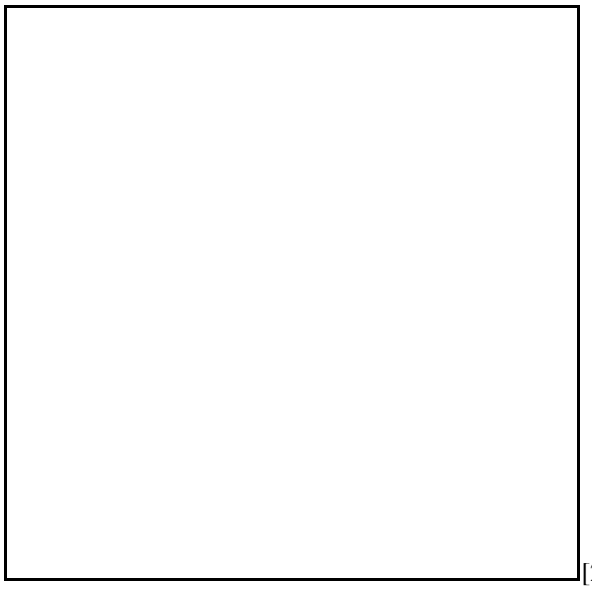
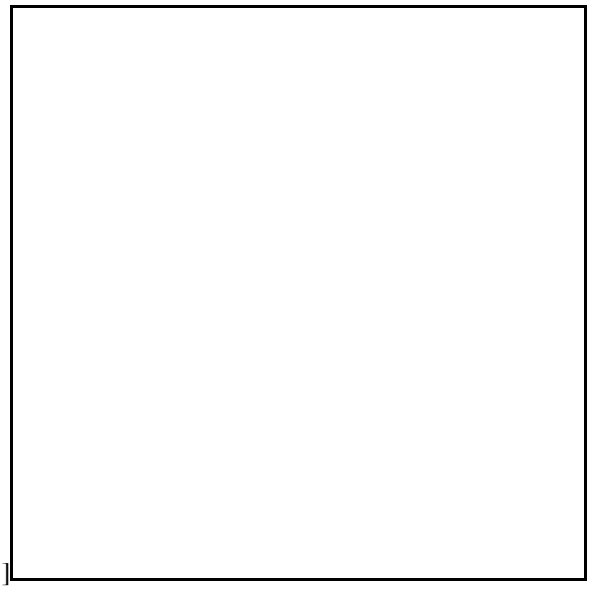
[21]. The current work uses the findings of Surks [16] to improve the performance of a circular ejector.

Although ejector designs have varied greatly in size and aspect ratios, general conclusions can be made for all ejectors. Most of the past literature on ejector designs has shown that the mixing of the inlet streams is the determining factor in the performance of steady flow ejector. Inlet pressure non-uniformity can provide significant improvements in mass entrainment and thus thrust augmentation. Mixing designs using large scale, low-loss, streamwise vorticity have been proven to be most effective. Although the mixing within the ejector is most critical, its design must be compact and light weight in order to be practical.

Experimental Apparatus

The experimental study was conducted at the Tufts University Fluids Laboratory. Both centerline velocity and mass entrainment measurements are used to calculate the improvement in ejector performance provided by the generators. The mass flux and centerline velocity measurements were obtained on an air jet using a stagnation probe.

Air Jet Facility

Two dimensional velocity profiles of both the jet exit and the ejector exit were used to calculate the mass flux entrained into the ejector. Air was supplied to the jet by a compressor, producing a plenum pressure, varying less than 6.5% per run, which was monitored constantly throughout each run. All velocity measurements were normalized by the instantaneous plenum pressure to minimize the effect of this drift. The flow enters the plenum through two air intake valves located opposite each other to reduce any swirling effects. The plenum is 28 jet diameters in length, and 8 jet diameters in diameter. Upon entering the plenum the air passes through a honeycomb and then a series of screens. Finally a fifth order polynomial contraction (64:1 area ratio) reduced the exiting diameter to 1.9 centimeters. Velocities ranging from 7.5 to 30 m/s were used to produce Reynolds numbers from 12,500 to 50,000. Figure 1 presents a schematic of this air jet facility.

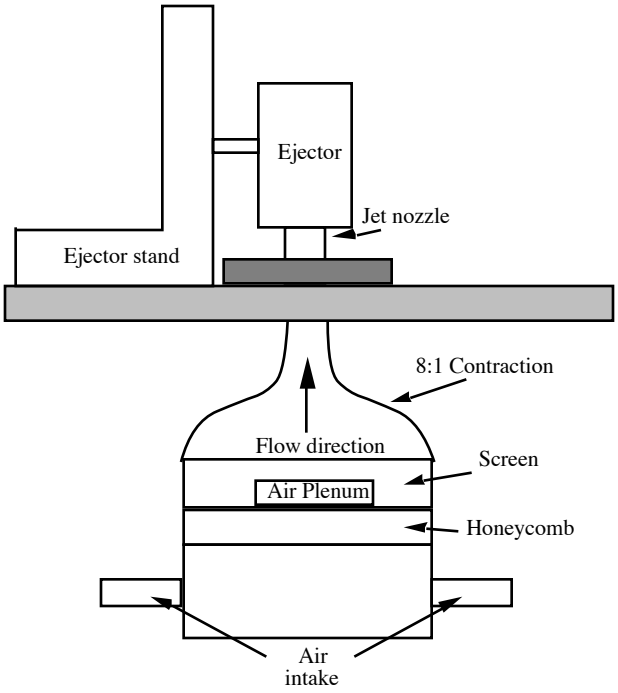

Figure 1 - Tufts air jet facility

Ejector Setup

Two primary nozzles were examined in our study. The first case, using the reference nozzle, has an axisymmetric jet issuing into the ejector shroud. The second case, with the vortex nozzle, is identical to the reference case except for of four triangular tabs or vortex generators at the nozzle exit.

Surks et al. [15,16] tested many different vortex generator configurations at a Mach number of 0.6 using image analysis and found that the "90° symmetric" case was the most effective at entraining ambient flow in a free jet. The vortex nozzle incorporates the generator configuration shown in figure 2. Using half delta-wing generators with a height of 0.15 jet diameters and a base length of 0.3 jet diameters, angled at a 30° angle of attack to the incoming flow, it

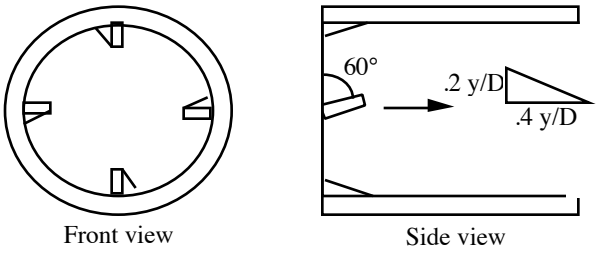

Figure 2 - Vortex nozzle generator orientation

produces an increased mass entrainment of 50% over that of an axisymmetric jet [15, 16].

The vortex nozzle consists of four vortex generators, positioned using the 90° symmetric configuration, in the primary nozzle leading into the jet ejector. A simple hollow cylinder is used for an ejector in order to isolate the effects of the generators and simplify the analysis. Once the effects of the vortex generators on mass entrainment are better understood, they can be used to further improve many other ejector inlet and outlet designs. Figure 3 shows how vortex generators can be implemented into a basic ejector design model.

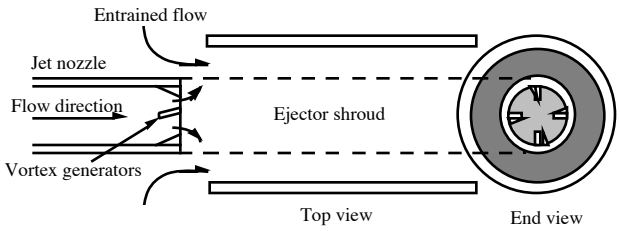

Figure 3 - Vortex generator implementation

The effect of the vortex generators on the performance of circular ejectors was evaluated for many shrouds varying in length (Le), diameter (De), and spacing (S). The parameters varied are shown in figure 4. The parameters examined in this study are normalized by the jet diameter (Dj) and are provided in Table 1. This analysis provided us with information on how the ejector size and position affects the improvement, due to the vortex generators, of ejector performance.

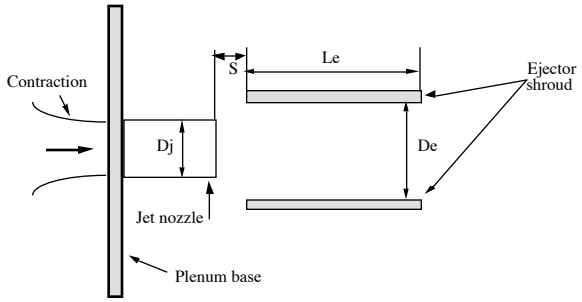

Figure 4 - Ejector parameters

Table 1 - Ejector parameters

Dimensionless Parameters	Cases Run
De/Dj	2,3,4
Le/Dj	4,6,10,12
S/Dj	-2,-1,0,1,2,3
Re	16,667-50,000

In order test the effect of these parameters on ejector performance, each parameter was individually varied while all other characteristics were held at standard dimensions. The "standard" ejector has a length of 6 jet diameters and a diameter of 2 jet diameters and is positioned flush with the jet exit at spacing of S=0. The baseline Reynolds number is 50,000.

Measurement Techniques and Analysis

Velocity Measurements in Air

In order to calculate the increase in mass entrainment produced by the ejector, Pitot static measurements were taken in a two dimensional grid at both the exit of the jet nozzle and the ejector . A two dimensional computerized

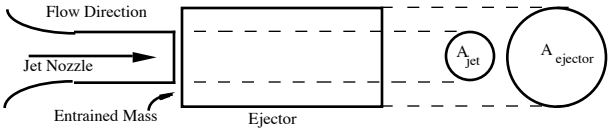

Figure 5 - Mass entrainment analysis

traversing mechanism was used to position the probe with an accuracy of 0.0125 mm. The velocity at each point in the profile was determined from an average of 1,000 samples taken over 1.5 seconds. Each point was normalized by a simultaneous plenum pressure measurement. Further, an ambient pressure reading was taken for each point in order to minimize effects of temperature drift. The probe was traversed in 0.127 cm increments. This step size was determined by choosing the largest step size which predicted a nozzle diameter, based on exiting mass flow rate, to within 1 percent.

In order to quantify the effectiveness of an ejector as a pumping mechanism, we have focused on the ejector's ability to entrain mass and thus increase pumping efficiency. Based on continuity and the sketch presented in figure 5, the mass flow rate through an ejector can be described as,

$$\dot{m}_{entrained} = \dot{m}_{ejector} - \dot{m}_{nozzle}. \qquad (1)$$

This defines the mass flow rate of entrained fluid as equal to the mass flow rate leaving the ejector minus the mass flow rate leaving the jet nozzle. After nondimensionalizing the mass entrainment by the mass flow rate of the jet and discretizing the equation for incompressible flow, equation 2 results

$$\frac{\dot{m}_{entrained}}{\dot{m}_{nozzle}} = \frac{\rho \sum \overline{U}_{ejector}(x,y)\Delta x \Delta y}{\rho \sum \overline{U}_{nozzle}(x,y)\Delta x \Delta y} - 1. \qquad (2)$$

Further, non-dimensionalizing by the corresponding plenum velocity , yields

$$\frac{\dot{m}_{entrained}}{\dot{m}_{nozzle}} = \frac{\sum \left[\overline{U_{ejector}} / U_{plen} \right](x,y)\Delta x \Delta y}{\sum \left[\overline{U_{nozzle}} / U_{plen} \right](x,y)\Delta x \Delta y} - 1. \qquad (3)$$

The final comparison we present is the increase in mass entrainment provided by the vortex generators. This improvement is defined as the difference in mass entrainment between the vortex and reference cases normalized by the amount of mass entrained in the reference case;

$$\left(\begin{matrix} mass\_entrainment \\ fraction(\eta) \end{matrix}\right) = \frac{\left[\dot{m}_{entrained} / \dot{m}_{nozzle}\right]_{vor}}{\left[\dot{m}_{entrained} / \dot{m}_{nozzle}\right]_{ref}} - 1. \quad (4)$$

All measurements of mass entrainment are normalized by the individual mass flux of the particular nozzle tested. The area of the jet nozzle varies significantly between the reference and vortex cases. Since the vortex nozzle has an effectively smaller area, its mass flux will correspondingly be lower. The frontal area of the vortex nozzle is approximately 11 percent less than that of the reference nozzle. This area discrepancy between the reference and vortex nozzle is due to the difference in the frontal blockage caused by the generators (see figure 6).

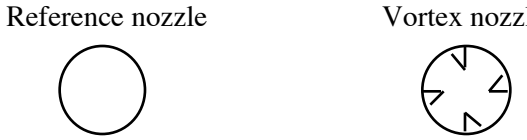

Figure 6 - Area disparity: reference vs. vortex nozzle

Measurement Uncertainties

Velocity

Since several measured velocity readings are needed to calculate the mass entrainment of the ejector, it is very important to minimize the uncertainty. The Pitot probe setup is connected to a MKS type 310CH-100 baratron. Each velocity reading is compared to the ambient pressure at the time of the measurement, producing a corrected velocity. This was done in an effort to force near zero velocity measurements outside of the ejector shroud, thus avoiding a compounding error produced by non zero velocity measurements in the ambient. A corrected zero velocity, which deviated less than .3% from zero when compared to the freestream velocity, was obtained.

In a comparison of several identical runs, done on different days, the repeatability of the centerline data is within less than 2 percent. The repeatability of the centerline profiles within the first 6 jet diameters downstream of the jet exit, however, is within less than 0.5%. Each velocity measurement is assumed to have a maximum error of 2% and referring to equation 4 this yields a maximum possible error of approximately 8% for the mass entrainment calculations.

Centerline Velocity Decay

The figures presented in this section show the decay of the geometric centerline velocity from the nozzle exit. The data is presented on contour plots showing the percent decrease in centerline velocity due to the vortex generators. The use of the contour plots allows for a clear and concise presentation of data which would be otherwise difficult to read if presented on standard centerline graphs.

Jet Flow - Centerlines Profiles

A standard axisymmetric jet, without an ejector, has a centerline velocity that begins decaying at approximately 4 jet diameters downstream of the nozzle (11,19). With the insertion of the vortex generators, in the 90° symmetric configuration, the decay of the centerline occurs much sooner, at approximately 2.5 jet diameters. The centerline velocity is unaffected by the generators until this point. This is illustrated in figure 7. The mixing of the round jet with the ambient results from the coherent characteristic structures in the jet shear layer and viscosity. The vortex nozzle, however, introduces large scale, streamwise structures which inviscidly stir the flow to increase the mixing.

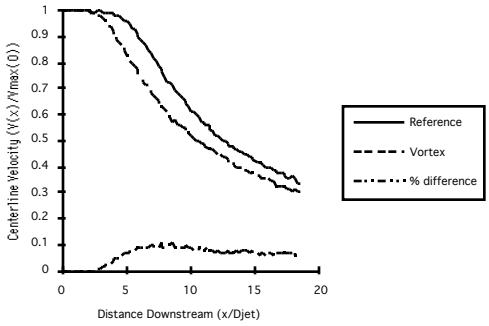

Figure 7 - Comparison of centerline velocity decay for nozzles without ejectors

Ejector Flow - Centerlines Profiles

A comparison of the centerline velocity decay through a standard ejector for the reference and vortex cases is shown in figure 8. This graph is in the conventional style for centerline plots. The vertical axis shows the centerline velocity of the jet flow at any position downstream normalized by the centerline velocity at the jet exit. The horizontal axis represents the distance downstream of the jet nozzle normalized by jet diameter. As in figure 7, the no ejector case, the decay of the centerline with the vortex nozzle occurs noticeably sooner than for the reference nozzle. The decay of the centerline for the reference ejector is similar in shape to that of the unshrouded axisymmetric jet shown in figure 7. The ejector shroud delays the onset of decay by a distance of 1.5 jet diameters downstream. In preventing the spread of the shear layer, the ejector acts as a shield preventing the potential core from mixing with the ambient fluid and delaying any significant decay until beyond the ejectors exit at 6 jet diameters downstream. In the vortex ejector the core velocity begins to deteriorate at the same location as the unshrouded nozzle, at 2.5 jet diameters downstream. The decay within the ejector shroud, however, becomes more gradual than in the no ejector case. The large scale mixing due to the vortex generators is unaffected by the presence of the ejector. However, the shear layer spreading is impeded by the ejector walls. At the ejector exit the centerline velocity of the vortex case has decreased 23% as compared to 1% for the reference nozzle due the increased mixing resulting from the additional streamwise vorticity introduced by the generators.

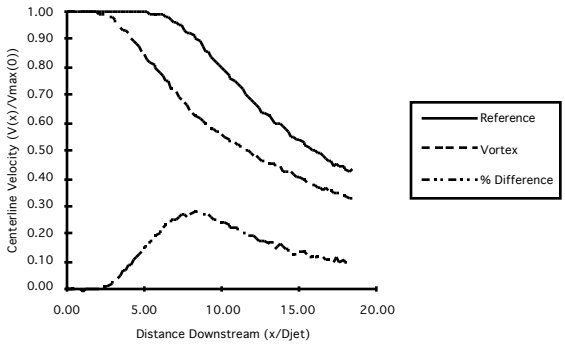

Figure 8 - Centerline decay for standard ejector

In an effort to simplify the presentation of the centerline data for parameter variation, contour plots showing the percent difference between the centerline decay of the reference and vortex cases will be used. The distance downstream of the jet exit is shown on the vertical axis, and the ejector parameter (e.g. diameter, length, or spacing) being varied is shown on the horizontal axis. The contour levels show the percent difference between the centerline velocity of the vortex and reference ejectors.

In the variation of ejector diameter, all other parameters are held constant. All of the ejectors have a standard length of 6 jet diameters, and are at a spacing of zero (the ejector entrance is flush with the jet nozzle exit). The effect of ejector diameter on the velocity decay of the potential core is illustrated in figure 9. Ejector diameter, shown on the x-axis, is varied between 2 and 4 jet diameters. The plot shows a linear interpolation between the diameters studied (2.0, 2.67, 3.33, 4.0). Within 2.5 jet diameters of the jet exit there is essentially no difference between the two cases. Inside the ejector shroud, up to 6 jet diameters downstream of the jet nozzle, the percent decrease in centerline velocity due to the vortex generators is independent of ejector diameter. In fact, the centerline decay for the vortex nozzle is essentially independent of ejector diameter. This again shows that the decay of the centerline is predominantly a result of the vortex mixing rather than shear layer spreading. The change in percent difference comes from the effect of diameter variation on the decay of the reference nozzle. Beyond the ejector exit the percent decrease in centerline velocity is much more significant for smaller diameter ejectors. This is because the smaller diameter ejectors allow less spreading of the shear layer in the reference cases.

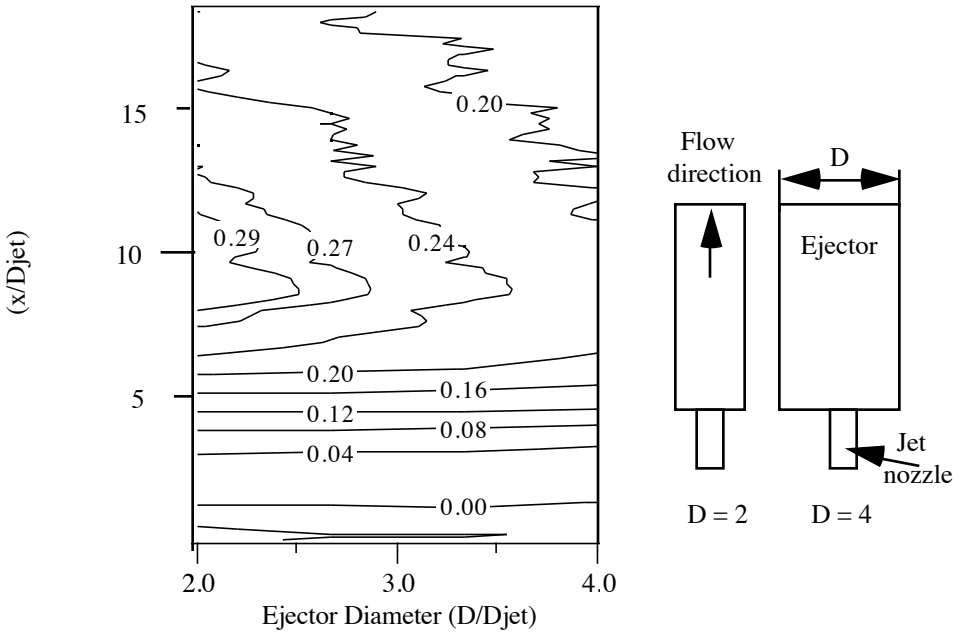

Figure 9 - Percent decrease in centerline velocity of vortex nozzle with diameter variation

Adjusting the length of the ejector, with diameter held at 2 jet diameters and a spacing of zero, has very little affect on the centerline velocity decay of either the reference or vortex cases within the first five jet diameters downstream. This is illustrated in figure 10, which shows the difference in centerline decay for a variation of ejector length from 0 to 12 jet diameters (equivalent to 0 to 6 ejector diameters). Only a slight deviation is shown for the no ejector case (L=0) which is due to the reference case decaying more rapidly due to the absence of the ejector shroud. Beyond 6 jet diameters downstream, the vortex generators have the greatest impact on the decay of the centerline velocity for ejector lengths between 4 and 8 jet diameters.

Centerline velocity decay for the reference case is delayed until the ejector's exit up to an ejector length of approximately 8 jet diameters, beyond which the decay begins within the ejector shroud. The decay of the centerline for the vortex nozzle begins within the ejector shroud, at approximately 2.5 jet diameters downstream of the jet exit, regardless of the length of the ejector, for the cases studied.

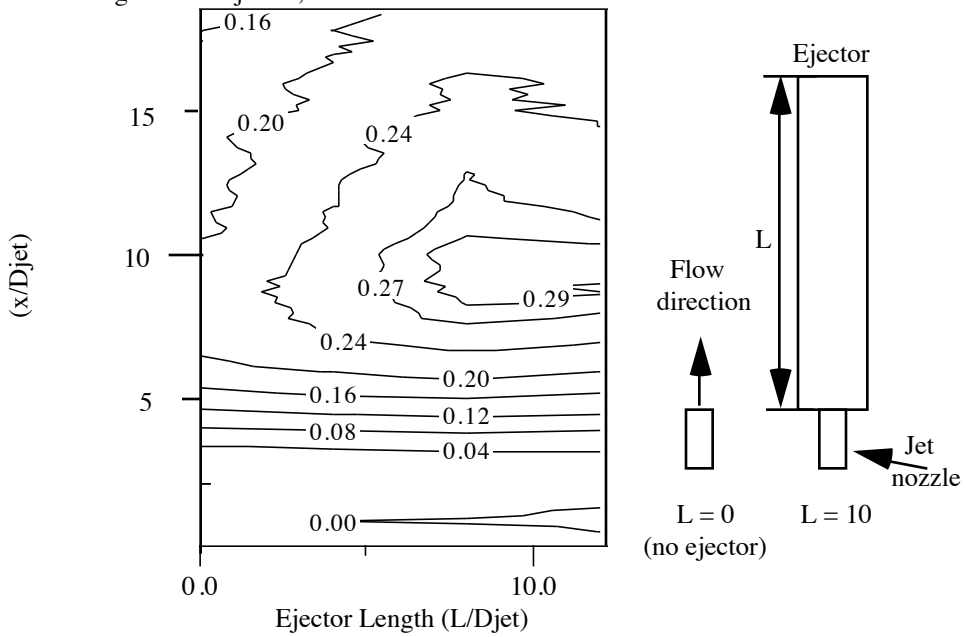

Figure 10 - Percent decrease in centerline velocity of vortex nozzle with length variation

Figure 11 is a contour plot illustrating the effect of varying ejector spacing on the percent decrease in centerline velocity of the vortex nozzle over the reference nozzle. The variation of position from, S=-2 to S=+3, of a standard ejector (L=6 and D=2) is shown on the horizontal axis. The decrease in centerline velocity is highly dependent on the downstream location of the ejector. The impact of the vortex generators is much stronger for an ejector of negative spacing, or as the ejector shroud is positioned such that it partially covers the exit of the primary jet. Since the entrainment of the reference nozzle is dependent on the viscous mixing of the shear layer, it is incapable of producing a pressure drop comparable to the vortex nozzle's stirring capabilities. It is important to point out that at an ejector spacing of S=-2 the beginning of the ejector shroud is almost flush with the plenum base (see figure 4), severely limiting the amount of mass entrainment in both cases.

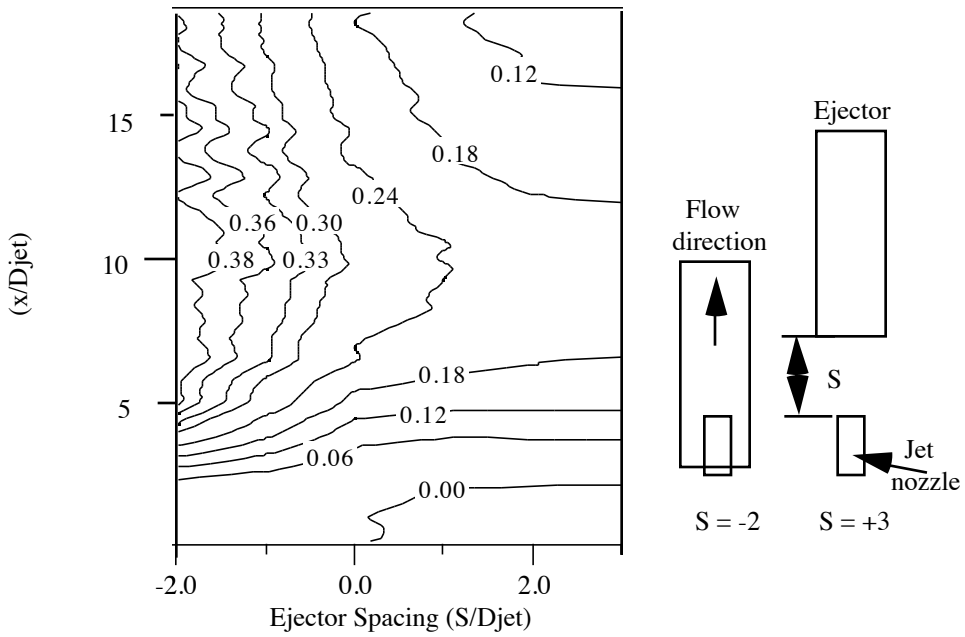

Figure 11 - Percent decrease in centerline velocity of vortex nozzle with spacing variation

Finally, figure 12 demonstrates the effect of jet Reynolds number. Once the jet becomes turbulent, the centerline decay through the ejector is not significantly dependent on the Reynolds number. For lower Reynolds numbers the decay of the centerline occurs slightly faster. Again the reference nozzle seems to be more affected by the variation than does the vortex case. The streamwise vorticity introduced to the flow stirs the ambient, low-speed, fluid into the potential core. This causes a much more rapid deterioration than the viscous spreading of the shear layer.

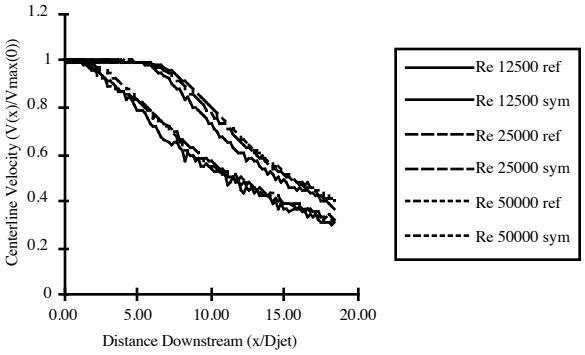

Figure 12 - Centerline decay of standard ejector case for varying Reynolds numbers

Although the decay of the centerline velocity is not the best indicator of ejector efficiency, it has provided insight to the effect of the vortex generators placed upstream of the ejector shroud. The centerline decay of the vortex nozzle is independent of the presence of the shroud. The rapid decay of the centerline velocity due to the generators implies that the flow exiting the ejector shroud is better mixed than in the reference case. By increasing the rate of mixing within the ejector shroud the pumping efficiency of the ejector will improve.

Mass Entrainment Measurements

Two-Dimensional exit profiles

Two dimensional profiles taken at the exit of the reference and vortex nozzles respectively are shown in the figure 13. The reference nozzle, an axisymmetric jet, has a uniform nondimensional velocity of 1, as is expected. Looking at the vortex nozzle, the size and location of the vortex generators are quite apparent. In order to determine the step size used in the traverse file for data acquisition, the diameter of the reference nozzle was determined and

compared to the actual value of 1.905 centimeters. A step size of .127 cm resulted in an error of less than 1 percent in the calculation of nozzle diameter, thus it was selected as the standard step size. The actual area of the reference nozzle is 2.85 cm^2, and the resulting area calculated from figure 13 is 2.80 cm^2, yielding a disparity of 1.7 percent. Using the same method of calculations for the vortex nozzle, the area minus the frontal blockage due to the generators was calculated to be 2.48.

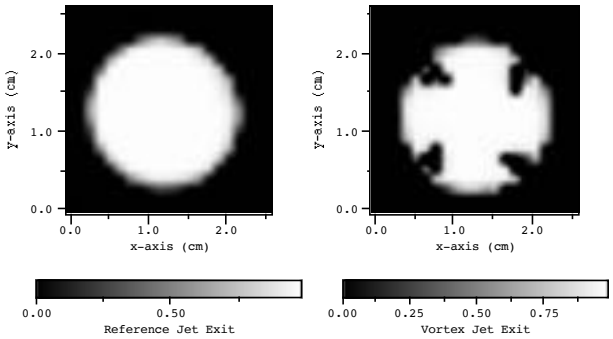

Figure 13 - Jet exit mass entrainment

Figure 14 presents a comparison between of dimensional velocity profiles of the reference and vortex nozzles taken at the ejector's exit. These profiles were taken at the exit of the standard ejector for each of the two cases. Each point on the following graphs is derived from the analysis of similar plots. This figure illustrates the distinct flow pattern generated by the vortex nozzle. The ejector on the left, the reference case, shows little spreading of the potential core. The center of the ejector has a velocity of nearly equal to that at the jet exit, and little mixing has occurred, since the velocity at the edge of the ejector is essentially zero. In the vortex nozzle, on the right, the dark region representing the potential core is spread out by the vorticity introduced by the generators. Although there is no region of velocity equal to that exiting the primary jet nozzle, the mixing enhancement due the generators has provided a more uniform velocity profile at the ejector exit. Notice that the velocity map of the vortex ejector exit is similar in shape to the vortex nozzle exit profile shown in figure 8.

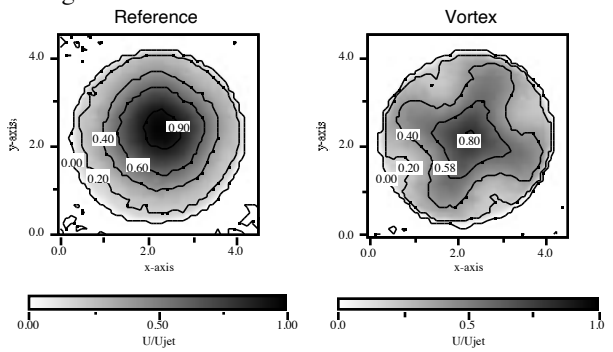

Figure 14 - Ejector exit velocity profile

Through the acquisition of two dimensional exit velocity profiles of both the jet nozzle and the ejector, the amount of mass entrained can be determined using equation 4. The following plots show, η, the increase in mass entrainment for each of the ejectors due to the introduction of the vortex generators to the jet nozzle.

Because the streamwise vortices generated by the vortex nozzle are more effective at entraining flow at the nozzle exit than are the natural coherent structures of the reference jet, there is an increase in the amount of mass entrained when the vortex nozzle is implemented. Figure 15 presents the mass entrainment of each nozzle, as well as the percent increase in mass entrainment of the vortex case over the reference case, as a function of ejector length. The shroud length is varied from 4 to 10 jet diameters. There is an increase in mass entrainment for both nozzles as the ejector shroud is lengthened. This increase becomes more gradual as the ejector length approaches 10 jet diameters. In general, longer ejectors are capable of entraining more mass, however, a larger ejector is inefficient as it must compensate for excess losses due to drag.

The improvements due to the generators are stronger for shorter length ejectors. Further, for shorter length ejectors, the increase in pumping performance due to the generators can exceed 30% . Beyond an ejector length of 6 jet diameters, there is a decrease in the mixing benefits of the generators with increase in ejector length. This again shows that most of the mixing improvement due to the generators occurs near the jet exit.

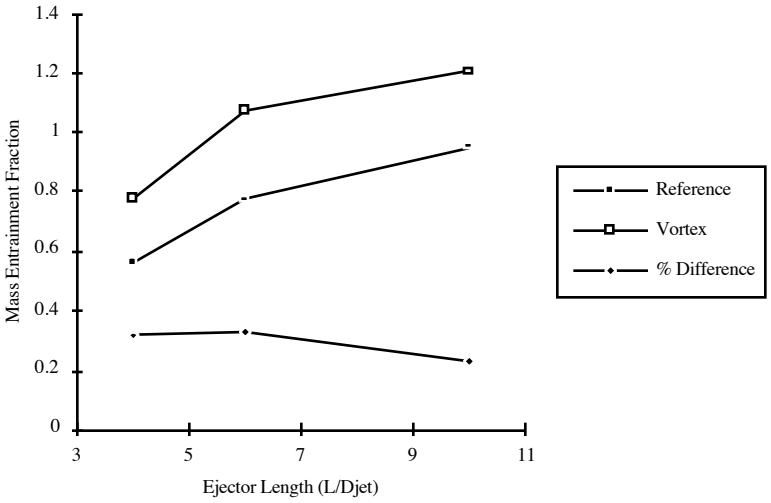

Figure 15 - Mass entrainment of reference and vortex cases versus ejector length

As the ejector is moved further downstream, the ejector becomes more efficient at entraining mass, however, the percent improvement due to the generators decreases. This decrease in percent improvement is illustrated in figure 16. The vortex nozzle is most effective for the negative spacings, due to the shorter mixing region. The percent improvement decreases with an increase in spacing. This trend is comparable to the data presented for length variations in figure 15. The mixing length of the ejector is defined as the distance from the exit of the jet nozzle to the exit of the ejector. The mixing length of the ejector for the S = -1 case is 5 jet diameters and the mixing length of the S = +3 case is 9 jet diameters for the standard ejector. When this data is compared to standard ejector data for lengths of 5 to 9, the data corresponds to within 5 percent. This shows that the entrainment capability of an ejector is a strong function of the length of the mixing region.

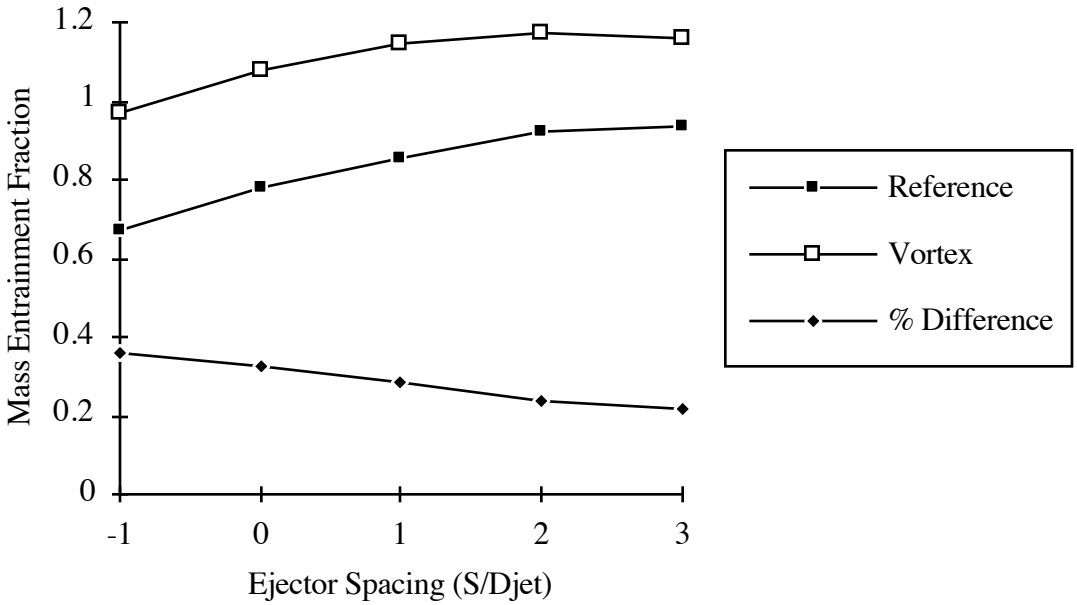

Figure 16 - Mass entrainment of reference and vortex cases versus ejector spacing

Figure 17 shows the change in mass entrainment for both the reference and vortex cases with a variation in Reynolds number. Within a variation of Reynolds number between 17,000 to 50,000, the reference case shows no difference in the amount of entrained mass. The vortex case, on the other hand, shows a slight increase in the amount of entrained mass with an increase in Reynolds number. This variation in mass entrainment, however, is much less than when the ejector's physical parameters are varied.

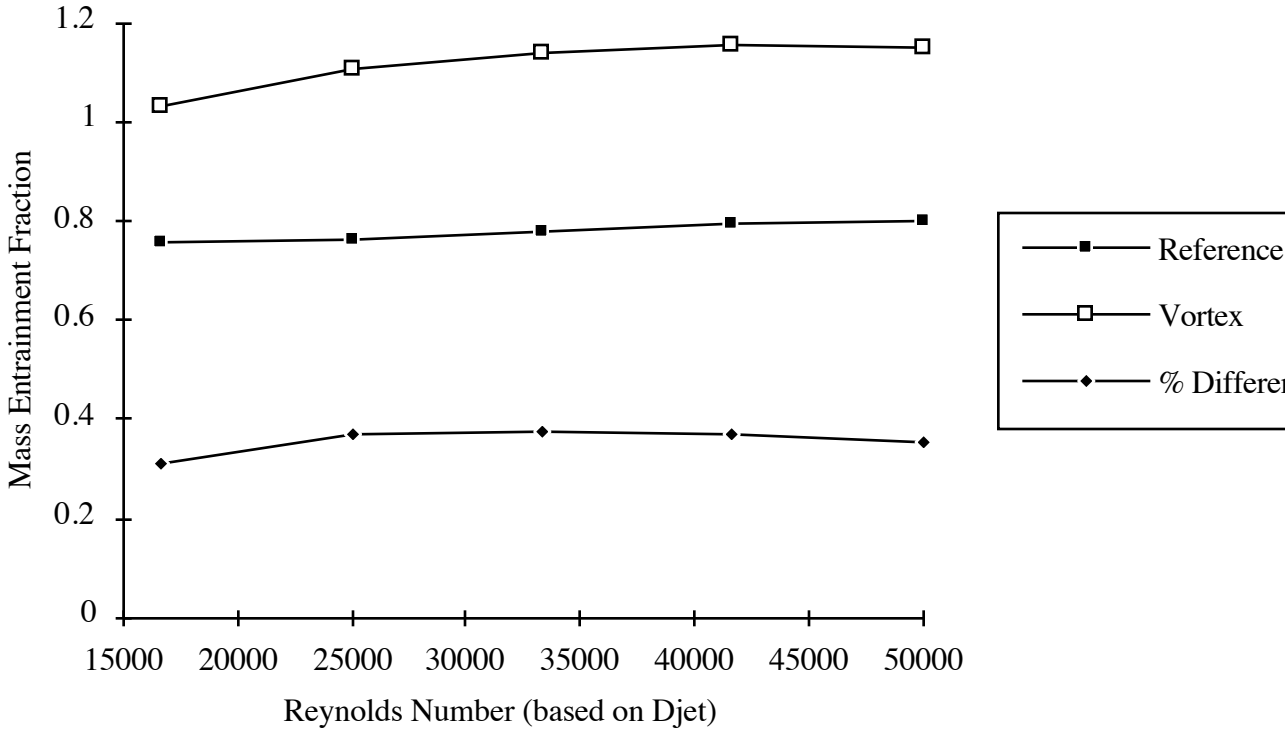

Figure 17 - Mass entrainment of reference and vortex cases versus Reynolds number

Conclusions

Through the addition of large-scale streamwise vorticity within the shroud, as much as a 35% improvement in ejector performance can be achieved. The vortex generators implemented, in the 90° symmetric configuration, upstream of an ejector shroud were shown to increase centerline decay, mass entrainment, and shear layer spreading within the ejector.

The decay of the centerline through the ejector occurs much quicker due to the presence of the vortex generator in the exit of the primary nozzle than without the generators. Further, the decay in the vortex case is essentially independent of ejector parameters; implying that the streamwise vorticity dominates.

The results presented on the mass entrainment of the vortex ejector show more than a 35 percent increase in mass entrainment due to the presence of the generators. Although the vortex cases always showed an improvement over the reference cases, the most attractive feature of the generators is that they show the greatest improvement over the reference case for smaller ejector parameters (e.g. ejector shroud length). This allows for the design of shorter more efficient ejectors.

Acknowledgments

The authors would like to thank both the McDonnell Douglas Corporation and Tufts University for funding this research project.

References

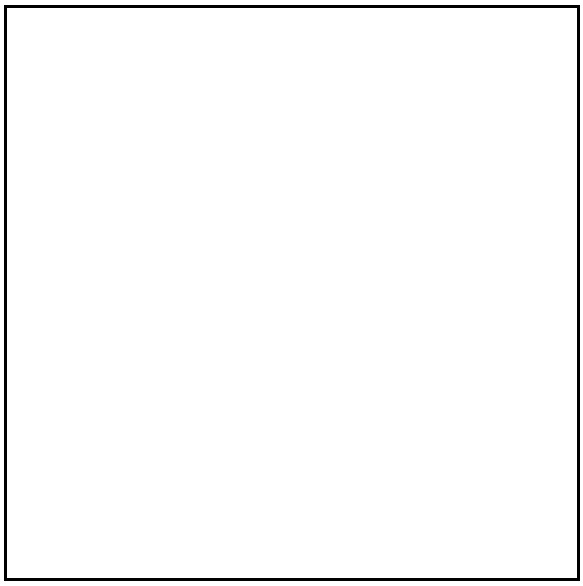

1. Presz, W.M.J. and E.M. Greitzer, *A Useful Similarity Principle for Jet Engine Exhaust system Performance*. AIAA Paper 88-3001, 1988.
2. Presz, W.M.J., B.L. Morin, and R.G. Gousy, *Forced Mixer Lobes in Ejector Designs*. AIAA Paper 86-1614, 1986.
3. Presz, W.M.J., B.L. Morin, and R.G. Gousy, *Forced Mixer Lobes in Ejector Designs*. Journal of Propulsion, 1988. **4**(4): p. 350-355.
4. Skebe, S.A., D.C. McCormick, and W.M.P. Jr., *Parameter Effects on Mixer-Ejector Pumping Performance*. AIAA Paper 88-0188, 1988.
5. Tillman, T.G., R.W. Paterson, and W.M.J. Presz, *Supersonic Nozzle Mixer Ejector*. Journal of Propulsion and Power, 1992. **8**(2): p. 513-519.
6. Bevilaqua, P.M., *Evaluation of Hypermixing for Thrust Augmenting Ejectors*. Journal of Aircraft, 1974. **11**(6): p. 348-353.
7. Bevilaqua, P.M. and J.K. McCullough. *Entrainment Method for V/Stol Ejector Analysis*. in *AIAA 9th Fluid and Plasma Dynamics Conference*. 1976. San Diego.
8. Mefford, L.A. and P.M. Bevilaqua, *Computer-Aided Design Study of Hypermixing Nozzles*. 1978, Naval Postgraduate School.
9. Chandrasekhara, M.S., A. Krothapalli, and D. Baganoff, *Mixing Characteristics of a Supersonic Multiple Jet Ejector*. AIAA Paper 87-0248, 1987.
10. Chandrasekhara, M.S., A. Krothapalli, and D. Baganoff, *Performance Characteristics of an Underexpanded Mulitple Jet Ejector*. Journal of Propulsion, 1990. **7**(3): p. 462-464.
11. Ho, C.-M. and E. Gutmark, *Vortex Induction and Mass Entrainment in a Small-Aspect-Ratio Elliptic Jet*. Journal of Fluid Mechanics, 1987. **179**: p. 383-405.
12. Wlezein, R.W. and V. Kibens, *Passive Control of Jets with Indeterminate Origins*. AIAA Journal, 1986. **24**(8): p. 1263-1270.
13. Longmire, E.K., J.K. Eaton, and C.J. Elkins. *Control of Jet Structures by Crown-Shaped Nozzle Attachments*. in *29th Aerospace Sciences Meeting*. 1991. Reno, Nevada.
14. Rogers, C.B. and D.E. Parekh, *Jet Mixing Enhancement and Noise Reduction by Streamwise Votrices*. AIAA Journal, 1992 submitted.
15. Surks, P., C.B. Rogers, and D.E. Parekh, *The Effect of Enhanced Streamwise on the Mixing and Acoustic Characteristics of an Air Jet*. AIAA Journal, 1993 submitted.
16. Surks, P., C.B. Rogers, and D.E. Parekh, *The Effect of Streamwise Vorticity on the Mixing and Acoustic Characteristics of an Axisymmetric Jet*. 1992, Tufts University.
17. Sammimy
18. Samminy
19. Lee, M. and W.C. Reynolds. *Bifurcating and Blooming Jets.* in *5th Symposium on Turbulent Shear Flows*. 1985. Ithica, New York.
20. Parekh, D.E., W.C. Reynolds, and M.G. Mungal, *Bifurcation of a Round Air Jet by Dual Mode Acoustic Excitation*. AIAA Paper 87-0164, 1987.

21. Wiltse, J.M. and A. Glezer, *Manipulation of Free Shear Flows Using Piezoelectric Actuators*. to appear in Journal of Fluid Mechanics, 1993.